Icarus 293 (2017) 172–179

Contents lists available at ScienceDirect

Icarus

journal homepage: www.elsevier.com/locate/icarus

The changing nature of rainfall during the early history of Mars

Robert A. Craddock[a,*], Ralph D. Lorenz[b]

[a] Center for Earth and Planetary Studies, National Air and Space Museum, Smithsonian Institution, Washington, D.C. 20560 United States
[b] Johns Hopkins University Applied Physics Laboratory, Laurel, MD. 20723 United States

ARTICLE INFO

Article history:
Received 15 September 2016
Revised 5 April 2017
Accepted 18 April 2017
Available online 21 April 2017

ABSTRACT

Several explanations have been proposed for the temporal differences in geologic processes associated with the modification of martian impact craters, which occurred throughout the Noachian, and the formation of valley networks, which occurred during the Noachian/Hesperian transition. Here we show that it could be a result of the changing nature of rainfall as the primordial atmospheric pressure on Mars waned through time. We calculate the terminal velocity and resulting kinetic energy from raindrops >0.5 mm in diameter that would impact the surface of Mars in a CO_2-rich atmosphere ranging in pressure from 0.5 to 10 bars. Our analyses indicate that the primordial atmosphere of Mars could not have exceeded ~4.0 bars as raindrop sizes would have been limited to <3 mm and surface erosion from rain splash and subsequent crater modification would not have occurred. At pressures between ~3.0 and 4.0 bars, sediment transport from rain splash could occur, but surface runoff would have been limited, which could explain the modification of impact craters. Once atmospheric pressures waned to ~1.5 bars, rainfall intensity could begin to exceed the infiltration capacity of most soils, which would be necessary to initiate martian valley network formation. Due to the lower gravity, a storm on Mars that occurred in a 1 bar atmosphere could generate raindrops with a maximum diameter of ~7.3 mm compared to 6.5 mm on the Earth. However, rainfall from such a storm would be only be ~70% as intense on Mars, primarily due to the lower martian gravity and resulting lower terminal velocities of the rain drops.

Published by Elsevier Inc.

1. Introduction

There is copious geologic evidence indicating that rainfall occurred during most of the early history of Mars, including the morphology of modified impact craters (Craddock et al., 1997; Craddock and Howard, 2002; Forsberg-Taylor et al., 2004; Howard, 2007; Matsubara et al., 2011), the characteristics of valley networks (Fassett and Head, 2008a; Irwin et al., 2011; Matsubara and Howard (2013); Matsubara et al., 2013), and fluvial sedimentary deposits analyzed by the Mars Pathfinder (Golombek et al., 1997), Opportunity (Grotzinger, 2013), and Curiosity landers (Williams et al., 2013). Modified impact craters (Fig. 1a,b) are ubiquitous features found throughout the Noachian highlands of Mars, including at higher latitudes (Craddock and Howard, 2002). Morphologic analyses of these craters indicate that a combination of both diffusional transport processes associated with rain splash and advective transport processes associated with surface runoff occurred (Craddock et al., 1997; Craddock and Howard, 2002; Forsberg-Taylor et al., 2004; Howard, 2007; Matsubara et al., 2011; Matsubara and Howard (2013)). Because modified craters are preserved in different stages of erosion and at different diameters, rainfall and surface runoff must have been operated throughout the Noachian as new craters continued to form (Craddock et al., 1997; Craddock and Howard, 2002; Howard, 2007).

In contrast, most valley networks (Fig. 1c) are concentrated around the equatorial area of Mars (e.g., Hynek et al., 2010) and have been age-dated to around the Noachian/Hesperian boundary (Hoke et al., 2011; Fassett and Head, 2008b). Morphologic studies show that when compared to terrestrial stream valleys martian valley networks typically have lower preserved drainage densities, shorter lengths, relatively constant widths, and low sinuosity (Cabrol and Grin, 2001; Irwin et al., 2011). Sharp divides between tributaries are rare, and most intervalley surfaces are poorly dissected (Fassett and Head, 2008a; Irwin et al., 2011). Valley topography is also poorly graded relative to nominally concave longitudinal profiles on Earth (e.g., Matsubara et al., 2013). Collectively, these observations indicate that valley networks represent immature drainage systems that did not fully integrate with the cratered landscape (Howard et al., 2005; Howard, 2007; Fassett and Head, 2008a; Irwin et al., 2011; Matsubara and Howard (2013); Matsubara et al., 2013). The development of large alluvial fans, the limited amount of breaching of for-

* Corresponding author.
E-mail addresses: craddockb@si.edu (R.A. Craddock), ralph.lorenz@jhuapl.edu (R.D. Lorenz).

http://dx.doi.org/10.1016/j.icarus.2017.04.013
0019-1035/Published by Elsevier Inc.

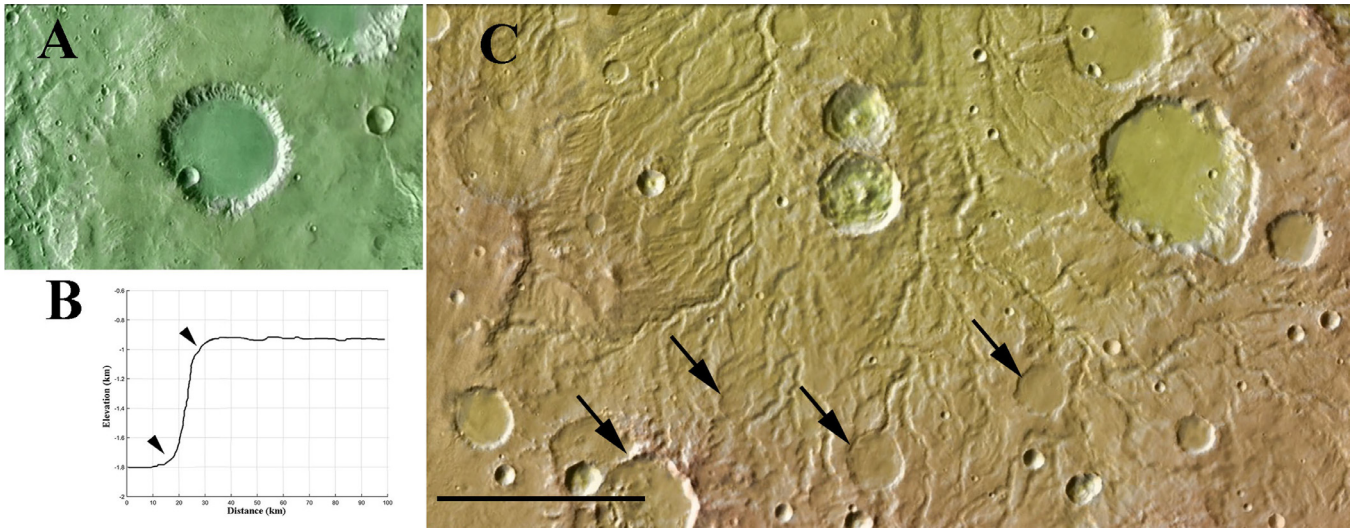

Fig. 1. A) An example of a typical modified impact crater on Mars. Although such craters are preserved in various stages of erosion, analyses of their morphologic characteristics indicates they were all modified by a combination of rain splash with limited amounts of surface runoff (Crater centered at −15.447° latitude, −16.353° longitude.) B) These morphologic characteristics can be seen in a cross-section of the crater topography based on Mars Orbiter Laser Altimetry (MOLA) data. The cross section shows the crater from the center outwards. The rounded rims and interior slopes (arrows) are particularly diagnostic of linear diffusional creep driven by rain splash. C) Valley networks also attest to surface runoff driven by rainfall. Their dendritic nature and deep valley incision coupled with evidence that water from the valley networks ponded within impact craters (arrows) indicate formation from precipitation and not snowmelt. (Figure is centered at 8.343° latitude, 47.951° longitude.).

merly enclosed drainage basins, and the style of entrenchment of rivers indicate that the environmental conditions supporting valley network formation were maintained for only a geologically brief period of time (Fassett and Head, 2008a; Irwin et al., 2011), perhaps in as little as 10^4–10^6 years (Moore and Howard, 2005). Thus, martian valley networks represent an epoch when erosion from surface runoff intensified, but only for a short period (Moore and Howard, 2005; Irwin et al., 2011; Matsubara and Howard (2013)).

The case for rainfall on a warm wet early Mars is not without controversy, particularly because many climate models have failed to explain how such conditions could occur if the “faint young sun” was only ~70% as luminous as it is today (e.g., Wordsworth et al., 2015). However, the geologic evidence is unequivocal. In addition to modified impact craters, valley networks, alluvial fans, and analyses of fluvial sediments at a variety of landing sites, large outflow channels (e.g., Baker, 1982), evidence for crater lakes (Goudge et al., 2016), intracrater lakes (Irwin et al., 2004), and a northern ocean (e.g., Carr and Head, 2003) attest to large bodies of liquid water on the surface, which is predicated by rainfall (Craddock and Howard, 2002). If precipitation were frozen (e.g., Wordsworth et al., 2015), climatic conditions would still have to have been able to support melting of large volumes of snow and ice, and under such conditions rainfall could occur (Craddock and Howard, 2002). In addition to the geologic evidence, multispectral detection of sulfates (e.g., Bibring et al., 2005) and phyllosilicates (e.g., Bishop et al., 2008) and their stratigraphic relationship can be explained if rain percolated through layers of basaltic rock (Zolotov and Mironenko, 2016). The implication from the collective evidence is that environmental conditions supporting crater modification were long-lived, but later these conditions changed so that surface runoff intensified (Craddock and Howard, 2002; Howard et al., 2005; Fassett and Head, 2008a; Irwin et al., 2011). It has been suggested that these changing conditions may be related to a decrease in the infiltration capacity of the regolith or a decrease in the rates of weathering and sediment production (Howard et al., 2005). Alternatively, however, the nature of the precipitation driving the erosion of the craters and subsequent valley networks may have changed (Howard et al., 2005). Here, the potential characteristics of rainfall under different possible atmospheric pressures are analyzed to better understand the climatic conditions and resulting geologic environment that may have occurred during the early history of Mars.

2. Approach

Soil erosion caused by rainfall is a major problem on Earth because it can often result in the breakdown and removal of the topsoil (e.g., Young and Wierma, 1973). In order to mitigate such problems, numerous studies have been conducted to understand the dynamics of rainfall and to quantify the amount of erosion that can take place during a storm (c.f. Springer, 1976). In general, the amount of erosion from rainfall is a function of the number and size of the raindrops, the velocity at which these drops impact the ground, and the characteristics of the soil. On Earth, the typical maximum size of raindrop is ~6.5 mm because aerodynamic forces cause larger drops to break apart (Komabayasi et al., 1964). The terminal velocity of such a large drop is ~8.5 m s^{-1}, while smaller drops fall more slowly. The variability in the sizes and velocities of raindrops influences the amount of erosion that occurs.

Empirical studies by Salles et al. (2000) have shown that there is a erosivity threshold, or critical kinetic energy, necessary to initiate soil detachment from the impact of a raindrop that is equivalent to 5 μJ for fine sand (D_{50} = 0.096 mm diameter particles) and 12 μJ for silt loam (D_{50} = 0.030 mm diameter particles). Higher values are required to detach silt loam because the mixture of smaller particles provides cohesion and increases the strength of the soil (Salles et al., 2000). Detachment of soil is also required to explain the diffusive component associated with the morphology of modified impact craters (Craddock et al., 1997; Craddock and Howard, 2002; Forsberg-Taylor et al., 2004; Howard, 2007; Matsubara et al., 2011), so the values for the critical kinetic energy can be used to assess the physical characteristics of raindrops that may have occurred on Mars.

A liquid drop in air quickly accelerates under gravity to a terminal velocity at which its weight is balanced by aerodynamic drag. The weight of a spherical drop varies as the cube of its diameter,

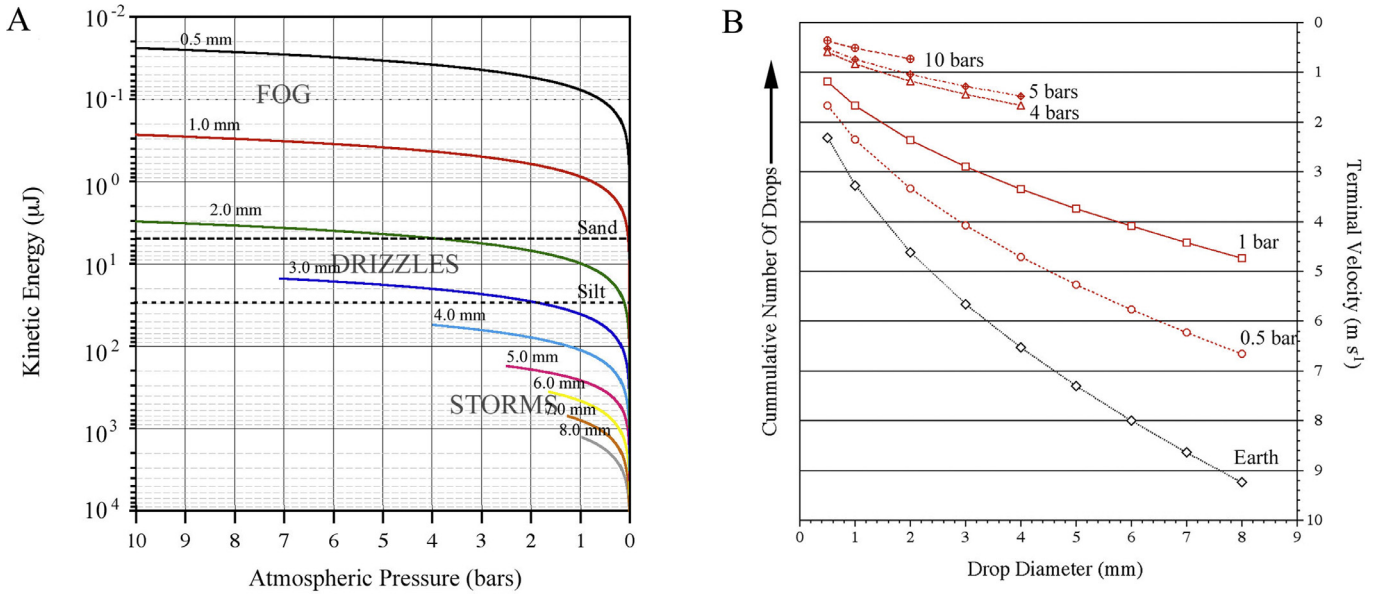

Fig. 2. A) Plot of the kinetic energy released by a raindrop upon impact as a function of drop diameter and atmospheric pressure. The threshold values necessary to initiate sediment transport of sand- and silt-sized particles (Salles et al., 2000) are shown for comparison. Note that larger diameter raindrops are not possible at higher atmospheric pressures. Because drop diameter can be related to rainfall intensity (Laws and Parson, 1943), the maximum raindrop sizes at different atmospheric pressures also reveals information about the possible scale of storms that may have occurred on Mars. B) Terminal velocity of individual raindrops as a function of size and atmospheric pressure. The terminal velocities of terrestrial raindrops of different sizes under normal conditions are shown for comparison. In a relative sense, the plot also shows the maximum drop size distribution at different atmospheric pressures based on empirical data (Laws and Parson, 1943; Marshall and Palmer, 1948).

whereas the cross-sectional area varies as the square of diameter, thus larger drops have a higher terminal velocity. Terminal velocity is written

$$v_t = (2mg/C_d\rho_\alpha A)^{1/2} \quad (1)$$

where m is the mass of the raindrop, g the acceleration due to gravity (3.75 m s^{-2} on Mars), C_d is the drag coefficient (a dimensionless quantity assumed here to be 1.0 for simplicity), ρ_a the atmospheric density, and A is the cross-sectional area of the raindrop. The resulting kinetic energy released by a raindrop that has reached terminal velocity can be calculated by the standard formula

$$\text{K.E.} = 1/2mv_{t^2} \quad (2)$$

In our calculations, the mass of the raindrop (m) varies as a function of drop size, and the terminal velocity (v_t) varies as a function of both drop size and atmospheric pressure.

3. Rainfall on Mars

To determine the terminal velocity of a raindrop on Mars, we considered a variety of raindrop diameters > 0.5 mm (Fig. 2). Similar to the early Earth, creating surface conditions on ancient Mars capable of supporting liquid water is complicated by the lower luminosity of the "faint young sun" (Sagan and Mullen, 1972). At a minimum atmospheric pressures higher than those present today would be required and proposed estimates range from 10 bars of CO_2 (Catling, 2009) to a minimum of 0.5 bars before atmospheric collapse occurs (Segura et al., 2008; Wordsworth et al., 2015). Potentially greenhouse gases, such as methane, ammonia, or sulfur dioxide may also be required (e.g., Segura et al., 2008). As shown in Table 1, the terminal velocities and corresponding kinetic energy of any raindrop of a given size would increase as the pressure of the early martian atmosphere decreased.

Another factor to consider is the maximum size of the raindrop that could be attained at any given atmospheric pressure. Although it is assumed that the shapes of the raindrops were spherical for simplicity, the actual shapes would vary as a function of size and atmospheric density. On Earth as raindrops become larger aerodynamic drag causes them to become prolate, and ultimately their bottoms flatten so the drops assumes a shape similar to the top of a hamburger bun (Reyssat et al., 2007). Then, as the size increases further the drop deforms into a sac (or umbrella) until aerodynamic drag eventually exceeds the surface tension causing the drop to fragment into smaller particles. Fragmentation begins when

$$v_t^2 d = \frac{8\gamma}{n\rho_\alpha C_d} \quad (3)$$

where d is the diameter of a sphere corresponding to the raindrop's volume, γ is surface tension on the raindrop (0.07286 N/m at 20 °C), and n relates the radius of the upper curvature of the drop to the spherical equivalent radius and is a factor between 1 and 2 (Matthews and Mason, 1964), following Lorenz (1993) we take the nC_d product to be equal to 1. Applying these parameters to water on the Earth yields a maximum drop size of 6.5 mm (Komabayasi et al., 1964), and when applied to methane on Titan it yields a maximum drop size of 9.5 mm (Lorenz, 1993). Atmospheric densities (ρ_α) between 10 and 0.5 bars yield maximum drop sizes ranging from 2.4 to 11.6 mm for Mars, respectively (Table 1). Under normal terrestrial conditions (1 bar, 20 °C), a raindrop on Mars could reach a maximum diameter of 7.3 mm, which is slightly larger than it would be on Earth, primarily because the lower gravitational acceleration on Mars results in a lower terminal velocity, thus allowing the drops to grow bigger. It can be shown that the dissolution of potential greenhouse gasses that may have been present in ancient martian atmosphere, such as NH_3 or SO_2, may yield drops of concentrated ammonia solution or sulfuric acid, but this would not change the surface tension or density of the raindrops enough to change the results by more than ~20% (e.g., Lange and Forker, 1967 pp. 1661–1665). A claimed dependence of surface tension on gravity (Weislogel et al., 1998) is tiny (0.5%) and was within the margin of error of the experiment, thus we use the standard value for water.

Table 1
Terminal velocities and kinetic energy associated with raindrops of different sizes under different atmospheric pressures on Mars. Energy values in red are incapable of initiating transport of sedimentary particles. Energy values in yellow are threshold values capable of initiating movement of sand-sized particles, but not silt. Transport can occur when values are in green.

Terminal Velocity ($m\ s^{-1}$) at 20°C	0.5 mm	1 mm	2 mm	3 mm	4 mm	5 mm	6 mm	7 mm	8 mm	Maximum Drop Size (mm)	Maximum v_t
0.5 bar	1.665	2.354	3.330	4.078	4.709	5.265	5.767	6.229	6.659	11.668	8.027
1.0 bar	1.181	1.671	2.363	2.894	3.342	3.736	4.093	4.421		7.317	4.520
4.0 bar	0.589	0.833	1.177	1.442	1.665					3.997	1.653
5.0 bar	0.523	0.739	1.045	1.280	1.478					3.909	1.461
10 bar	0.364	0.515	0.728							2.417	0.801
Terminal Velocity ($m\ s^{-1}$) on Earth	2.309	3.266	4.619	5.657	6.532	7.303	8.000	8.641			
Energy (μJ)											
0.5 bar	0.109	1.233	13.947	57.652	157.796	344.573	652.252	1118.741	1785.259		
1.0 bar	0.077	0.875	9.898	40.912	111.978	244.521	462.861	793.897			
4.0 bar	0.000	0.001	4.932	20.386	55.797						
5.0 bar	0.034	0.387	4.378	18.097							
10 bar	0.024	0.270	3.051								
Energy (μJ) Earth	0.151	1.710	19.347	79.972	218.888	477.978	904.778	1551.871	2476.439		

The maximum size of a raindrop is somewhat of a statistical concept since it is dependent on ambient conditions such as turbulence (Komabayasi et al., 1964), and disruption of the raindrop is not instantaneous (Laws and Parsons, 1943). However, measurements of raindrop size distributions show that sizes increase monotonically so that as the maximum raindrop diameter increases so do the sizes of all the other raindrops (Marshall and Palmer, 1948; Shin et al., 2015).

A variety of methods have been proposed to relate drop size to rainfall intensity (R). Perhaps the most widely used is the two-parameter exponential distribution function (e.g., Marshall and Palmer, 1948; van Dijk et al., 2002) where the relationship between rainfall intensity (I) to the median raindrop size (D_{50}) is expressed as

$$D_{50} = \alpha I^{\beta} \quad (4)$$

Here the coefficient α (in h) has reported values ranging from 0.80 in Poona, Italy (Kelkar, 1959) to 1.28 in Washington, DC (Laws and Parsons, 1943) and the coefficient β has reported values ranging from 1.23 in Amazonia, Brazil (Brandt, 1988) to 2.92 in Firenze, Italy (Zanchi and Torri, 1980). Although the median drop size (D_{50}) is typically skewed to smaller diameters, particularly at lower rainfall intensities (e.g., Springer, 1976), for simplicity we assumed it to be approximately half of the calculated maximum drop size under different atmospheric conditions as presented in Table 1. That is to say, we assumed a normal distribution of raindrop sizes with a median value equivalent to half of the calculated maxi-

Table 2
Estimated rainfall intensities on Mars at different atmospheric pressure. The median drop size is estimated to be half the calculated maximum drop sizes presented in Table 1. A range of known values for α and β are considered based on terrestrial literature (see text). Note that heavier rainfall intensities occur at lower atmospheric pressures. Classification of light rain (light green) and moderate rain (darker green) follow Kittredge (1948).

Pressure (bar)	Maximum Drop Size (mm)	Median Drop Size (mm)	Rainfall Intensity (mm h^{-1})			
			α=0.80, β=1.23	α=1.28, β=1.23	α=0.80, β=2.92	α=1.28, β=2.92
0.5	11.7	5.8	5.03	3.43	1.97	1.68
1	7.3	3.7	3.44	2.35	1.68	1.43
4	4.0	2.0	2.10	1.44	1.37	1.16
5	3.9	2.0	2.07	1.41	1.36	1.16
10	2.4	1.2	1.40	0.95	1.15	0.98

	Rainfall Intensity (inches h^{-1})			
	α=0.80, β=1.23	α=1.28, β=1.23	α=0.80, β=2.92	α=1.28, β=2.92
Light Rain				
Moderate Rain	0.20	0.14	0.08	0.07
	0.14	0.09	0.07	0.06
	0.08	0.06	0.05	0.05
	0.08	0.06	0.05	0.05
	0.06	0.04	0.05	0.04

mum drop size. This allows us to approximate potential rainfall intensities for Mars. Table 2 shows that under most conditions the rainfall intensities calculated using Eq. 4 would be 1.0–3.4 mm h^{-1}, which is characteristic of "light rain" (Kittredge, 1948). Heavier "moderate rain" of 3.4 mm h^{-1} or greater (Kittredge, 1948) could occur at atmospheric pressures of 1 bar or less. Obviously, there are a number of tacit assumptions involved with this approach. For example, α has been found to change as a function of air temperature (van Djik et al., 2002), and only normal conditions are assumed. It is possible there were a range of temperatures on Mars that could have changed seasonally and with latitude. It is also unknown if Eq. 4 can be applied to rainfall intensities exceeding 70 mm h^{-1}, so it is not clear if this approach is applicable to heavier rainfall events or storms (van Djik et al., 2002). Finally, it is also not known how Eq. 4 may be influenced by elevation or–as in the case of ancient Mars–different atmospheric pressures.

An alternative and more general approach to is to relate the drop size distribution (DSD) of a storm to rainfall intensity (I) by the equation

$$I = 3.6\frac{\pi}{6}\sum_i X(D_i)D_i^3 \quad (5)$$

where D_i is the diameter of the raindrop (cm) and $X(D_i)$ is the number of drops with diameter D_i arriving per unit time and per unit area (Lull, 1959). Naturally, larger storms generally have larger size raindrops and are more intense. Fog, for example, has a median drop diameter of 0.01 mm, a drizzle has a median drop diameter of ~1 mm, light rain is ~1.25 mm, and a thunderstorm (i.e., cloudburst) has a median drop diameter ranging from ~3 to 6 mm (e.g., Kittredge, 1948). There are a number of variables to consider, such as ambient conditions, how fragmentation may be affected on Mars, and the variability of the DSD between different storms. However, assuming a typical terrestrial thunderstorm and normal conditions the diameters of the raindrops (Di) would be slightly larger on Mars (~110%), but the number of drops arriving per unit time ($X(D_i)$) would be lower due to their slower terminal velocities (~50% relative to raindrop size). Thus, if an identical thunderstorm

were to occur on Mars, the resulting rainfall intensity (I) would only be ~70% the terrestrial value.

A key unknown in planetary geomorphic evolution is the nature of storms – whether a total annual rainfall is manifested as steady drizzle with small, non-eroding drops or as rare but intense storms. The case of Saturn's moon Titan is instructive here: early work (Lorenz, 1993) noted that in Titan's low gravity and thick atmosphere, methane raindrops would fall slowly (~1.6 m/s, similar to snowflakes on Earth) and would therefore be only weakly erosive (Lorenz and Lunine, 1996) and the total rainfall amount on Titan was expected to be small due to the modest sunlight driving convection. However, desert areas on Earth also receive little rainfall overall, yet can be geomorphologically dominated by fluvial processes and by analogy (Lorenz, 2000) it was cautioned well before Cassini's close examination of Titan that' most rivers on Titan may run dry, but river valleys may nevertheless be abundant and deep', a scenario that appears to have been borne out by Cassini-Huygens observations (Perron et al., 2006; Black et al., 2012; Langhans et al., 2012; Burr et al., 2013). The fact that even in Titan's low gravity, the energy per drop (Table 1) exceeds the 12 mJ terrestrial silt erosion threshold supports our use of this value in considering Mars. Titan's rainstorms appear to be relatively rare, but mesoscale cloud-convection simulations suggest (Tokano et al., 2001; Hueso and Sánchez-Lavega, 2006; Barth and Rafkin, 2007;) that large amounts (10 s of cm) of rainfall may be deposited in a few hours in a single event, and indeed that the violent ' microburst' outflows from such storms may be instrumental in contributing to the formation of aeolian landforms (Charnay et al., 2015).

4. Discussion

While the qualitative correlation of rain intensity and drop size is likely to hold at Mars, the different atmospheric structure and other parameters at Mars may be quantitatively different, so the above results should be considered with some caution. Nonetheless, another correlation is likely to be robust, namely the strong relationship of rainfall intensity (the instantaneous rain rate) to the column water vapor content of the atmosphere. The strength of convection permitting raindrop growth in a storm depends on the Convective Available Potential Energy (CAPE), which in turn depends on specific humidity; similarly, the total amount of rainfall is obviously limited by the atmospheric water vapor content. Empirical correlation shows (e.g. Muller et al., 2009) that precipitation rate increases strongly above a critical value of about 60 mm H_2O. Landscape modification by rainfall suggests then that such water vapor abundances occurred on Mars

Valley network formation is evidence for significant surface runoff (Howard et al., 2005; Howard, 2007; Fassett and Head, 2008a; Irwin et al., 2011; Matsubara et al., 2013), which would not occur until the rainfall intensity was capable of exceeding the infiltration capacity of the martian soil. It is estimated that rainfall intensities of 12.50–25.00 mm h^{-1} are needed to exceed the infiltration capacity of sandy soils, 2.50–12.50 mm h^{-1} for loams, clay, and silt, and 2.50–1.00 mm h^{-1} for clays and clay loams (Committee on Engineering Surveying of the Surveying Engineering Division of ASCE, 1985). These are typical soil types found on Earth. Determining the typical soil types that may have been present on early Mars is highly uncertain. However, multiple lines of evidence indicate that the surface of Mars is composed primarily of basalt (e.g., Craddock and Golombek, 2016), which would generate Andisols that are often coarse-grained (Neris et al., 2013) with extremely high infiltration capacities (> 130 mm h^{-1}; Jimènez et al., 2006). As an example, analyses of gully formation in the Keanakāko'i tephra, an Andisol resulting from explosive eruptions associated with Kilauea volcano in Hawaii, indicate that runoff occurs in events where rainfall intensity exceeds ~40 mm h^{-1} (Craddock et al., 2012). However, Andisols weather quickly, and their clay content has been seen to increase linearly over time (Slate et al., 1991), resulting in corresponding changes in the hydrologic properties of the soils. For example, Lohse and Deitrich (2005) found that an Andisol situated on 300 ya old basaltic bedrock in Hawaii was coarse-grained with a high hydraulic conductivity (36 cm h^{-1}). In contrast, a 4.1 Ma Oxisol (i.e., a highly weathered Andisol) was deep with a plinthite layer that overlaid several clay-rich soil horizons. The hydraulic conductivity of this older soil was three orders of magnitude lower (~0.01 cm h^{-1}), and Lohse and Deitrich (2005) determined that there was a high probability that average rainfall events recorded in the area would exceed the infiltration capacity of this older soil.

The implications for Mars is that young surfaces, such those created following the formation of an impact crater, would have an initially high infiltration capacity that would not be conducive to surface runoff unless rainfall intensity was extremely high. In contrast, however, the coarse-grained nature of the young crater ejecta would make it easier to move by rain splash as suggested from the experiments of Salles et al., (2000). Eventually rain and atmospheric moisture would breakdown this material, the particle sizes would decrease, the clay content would increase, and the infiltration capacity of the soil would be greatly reduced, thus enhancing the potential for surface runoff. This would suggest that a general decrease in the infiltration capacity of the martian regolith over time could initiate valley network formation, which is one of the scenarios proposed by Howard et al., (2005). However, new impact craters continue to form on Mars even today, and these craters generate fresh soil (i.e., young Andisols). While it is likely individual craters weathered over time, the resulting influence on runoff enhancement would have been local and confined to an individual crater and its ejecta. It is also important to note that weathering rates are influenced by the amount of moisture present, and soils in wetter environments generally weather faster (e.g., Kittredge, 1948). Basically, it is possible that changes in the infiltration capacity of the martian regolith over time had some influence in the onset of valley network formation. However, these changes would have also been influenced by the nature of martian rainfall and the corresponding climate. Given that impact craters continued to form over time, these effects would have been highly spatially variable as well. A change in the nature of rainfall during the history of early Mars appears to be the best solution for the observed temporal differences between the style of erosion during the Noachian as represented by modified impact craters (e.g., Craddock and Howard, 2002) followed by more enhanced erosion during the Noachian/Hesperian transition as typified by valley networks (Howard et al., 2005; Howard, 2007; Fassett and Head, 2008a; Irwin et al., 2011; Matsubara and Howard (2013); Matsubara et al., 2013).

5. Summary

The analyses presented here show that terminal velocities of individual raindrops would be generally incapable of releasing enough kinetic energy to initiate particle movement if the primordial martian atmospheric pressure exceeded ~4 bars as it would result in a maximum raindrop size of only ~3 mm (Fig. 2). Essentially at such high atmospheric pressures any rainfall on Mars would be equivalent to fog on Earth, and crater modification would not occur. At atmospheric pressures between ~3 and 4 bars, however, the terminal velocities and drop sizes begin to increase and the kinetic energy released by individual drops becomes sufficient to initiate movement of both sand- and silt-sized particles. At these lower pressures martian rainfall would be equivalent to drizzles or light rain on the Earth and crater modification would become more efficient. Beginning at ~1.5 bars the raindrop sizes

and associated kinetic energy reaches an optimum. The intensity of rainfall at such atmospheric pressures would be equivalent to storms on the Earth, and the intensity of such events would continue to increase until the atmosphere collapsed at ~0.5 bars. Such a scenario matches the temporal history of water on Mars as recorded by geologic features. In view of the evidence for rainfall (Som et al., 2012; Kavanagh and Goldblatt, 2015 and surface runoff (Nutman et al., 1997) for the early Earth, which has often been destroyed by subsequent erosion and plate tectonics, the surface of Mars may preserve a better geologic record of the evolution of the primordial atmosphere and the landscape that resulted after ocean formation occurred on our own planet. Consideration of this geologic history must be given when evaluating any model of the ancient climate of Mars.

Acknowledgments

The authors wish to thank Alan Howard, Ross Irwin and Sanjoy Som for providing comments on the original version of this manuscript. We also thank the two anonymous reviewers for their assistance. This research was supported by NASA Planetary Geology and Geophysics Research Grant NNX14AN32G; RL acknowledges the support of NASA grant NNX13AH14G.

References

Baker, V.R., 1982. The Channels of Mars. Texas University Press, Austin, p. 198.
Barth, E.L., Rafkin, S.C., 2007. TRAMS: a new dynamic cloud model for Titan's methane clouds. Geophys. Res. Lett. 34 (3). doi:10.1029/2006GL028652.
Bibring, J.-P., Langevin, Y., Gendrin, A., Gondet, B., Poulet, F., Berthé, M., Soufflot, A., Arvidson, R., Mangold, N., Mustard, J., Drossart, P., 2005. Mars surface diversity as revealed by the OMEGA/Mars express observations. Science 307, 1576–1581.
Bishop, J.L., NOE Dobrea, E.Z., McKeown, N.K., Parente, M., Ehlmann, B.L., Michalski, J.R., Milliken, R.E., Poulet, F., Swayze, G.A., Mustard, J.F., Murchie, S.L., Bibring, J.-P., 2008. Phyllosilicate diversity and past aqueous activity revealed at Mawrth Vallis, Mars. Science 321, 830–833.
Black, B.A., Perron, J.T., Burr, D.M., Drummond, S.A., 2012. Estimating erosional exhumation on Titan from drainage network morphology. J. Geophys. Res.-Planets 117 (E8). doi:10.1029/2012JE004085.
Brandt, C.J., 1988. The transformation of rainfall energy by a tropical rain forest canopy in relation to soil erosion. Journal of Biogeography 15, 41–48. doi:10.2307/2845044.
Burr, D.M., Perron, J.T., Lamb, M.P., Irwin III, R.P., Collins, G.C., Howard, A.D., Sklar, L.S., Moore, J.M., Ádámkovics, M., Baker, V.R., Drummond, S.A., 2013. Fluvial features on Titan: insights from morphology and modeling. Geol. Soc. Am. Bull. 125 (3-4), 299–321.
Cabrol, N.A., Grin, E.A., 2001. Composition of the drainage network on early Mars. Geomorphology 37, 269–287.
Carr, M.H., Head III, J.W., 2003. Oceans on Mars: an assessment of the observational evidence and possible fate. J. Geophys. Res. 108 (E5), 5042.
Catling, D.C., 2009. In: Gornitz, V. (Ed.), Atmospheric Evolution, Mars, in Encyclopedia of Paleoclimatology and Ancient Environments. Springer, New York, pp. 66–75.
Charnay, B., Barth, E., Rafkin, S., Narteau, C., Lebonnois, S., Rodriguez, S., Du Pont, S.C., Lucas, A., 2015. Methane storms as a driver of Titan/'s dune orientation. Nat. Geosci. 8 (5), 362–366.
Committee on Engineering Surveying of the Surveying Engineering Division of ASCE, 1985. Engineering Survey Manual. American Society of Civil Engineering, New York, p. 262. *no. 64*.
Craddock, R.A., Maxwell, T.A., Howard, A.D., 1997. Crater morphometry and modification in the Sinus Sabaeus and Margaritifer Sinus regions of Mars. J. Geophys. Res. 102, 13321–13340.
Craddock, R.A., Howard, A.D., 2002. The case for rainfall on a warm, wet early Mars. J. Geophys. Res. doi:10.1029/2001JE001505.
Craddock, R.A., Howard, A.D., Irwin III, R.P., Tooth, S., Williams, R.M.E., Chu, P.-S., 2012. Drainage network development in the Keanakāko'i tephra, Kīlauea Volcano, Hawai'i: Implications for fluvial erosion and valley network formation on early Mars. J. Geophys. Res. 117, E08009. doi:10.1029/2012JE004074.
Craddock, R.A., Golombek, M.P., 2016. Characteristics of terrestrial basaltic rock populations: Implications for Mars lander and rover science and safety. Icarus 274, 50–72.
Fassett, C.I., Head III, J.W., 2008a. Valley network-;fed, open-;basin lakes on Mars: distribution and implications for Noachian surface and subsurface hydrology. Icarus 198, 37–56.
Fassett, C.I., Head III, J.W., 2008b. The timing of Martian valley network activity: constraints from buffered crater counting. Icarus 195, 61–89. doi:10.1016/ j.icarus.2007.12.009.
Forsberg-Taylor, N.K., Howard, A.D., Craddock, R.A., 2004. Crater degradation in the martian highlands: morphometric analysis of the Sinus Sabaeus region and simulation modeling suggest fluvial processes. J. Geophys. Res. 109, E05002. doi:10.1029/2004JE002242.
Golombek, M.P., Cook, R.A., Economou, T., Folkner, W.M., Haldemann, A.F.C., Kallemeyn, P.H., Knudsen, J.M., Manning, R.M., Moore, H.J., Parker, T.J., Rieder, R., Schofield, J.T., Smith, P.H., Vaughan, R.M., 1997. Overview of the Mars Pathfinder mission and assessment of landing site predictions. Science 278, 1743–1748.
Goudge, T.A., Fassett, C.I., Head, J.W., Mustard, J.F., Aureli, KL., 2016. Insights into surface runoff on early Mars from paleolake basin morphology and stratigraphy. Geology 44 (6). doi:10.1130/G37734.1.
Grotzinger, J.P., 2013. Analysis of surface materials by the curiosity Mars rover. Science 341 (6153), 1475.
Hoke, M.R.T., Hynek, B.M., Tucker, G.E., 2011. Formation timescales of large martian valley networks. Earth Planet. Sci. Lett. 312, 1–12.
Howard, A.D., 2007. Simulating the development of Martian highland landscapes through the interaction of impact cratering, fluvial erosion, and variable hydrologic forcing. Geomorphology 91, 332–363.
Howard, A.D., Moore, J.M., Irwin III, R.P., 2005. An intense terminal epoch of widespread fluvial activity on early Mars: 1. valley network incision and associated deposits. J. Geophys. Res. 110, E12S14.
Hueso, R., Sánchez-Lavega, A., 2006. Methane Storms and Rain on Titan's Atmosphere from Numerical Simulations. Bulletin of the American Astronomical Society 38, 544.
Hynek, B.M., Beach, M., Hoke, M.R.T., 2010. Updated global map of martian valley networks and implications for climate and hydrologic processes. J. Geophys. Res. 115, E09008.
Irwin III, R.P., Craddock, R.A., Howard, A.D., Flemming, H.L., 2011. Topographic influences on development of martian valley networks. J. Geophys. Res. 116, E02005.
Irwin III, R.P., Howard, A.D., Maxwell, T.A., 2004. Geomorphology of Ma'adim Vallis, Mars, and associated paleolake basins. J. Geophys. Res. 109, E12009. doi:10.1029/2004JE002287.
Jimènez, C.C., Tejedor, M., Morillas, G., Neris, J., 2006. Infiltration rate in andisols: effect of changes in vegetation cover (Tenerife, Spain). J. Soil Water Conserv. 61 (3), 153–158.
Kavanagh, L., Goldblatt, C., 2015. Using raindrops to constrain past atmospheric density. Earth Planet. Sci. Lett. 413, 51–58.
Kelkar, V.N., 1959. Size distribution of raindrops-Part II. Indian Journal of Meteorology and Geophysics 4, 323–330.
Kittredge, J., 1948. Forest Influences. Dover Publications, New York, p. 394.
Komabayasi, M., Gonda, T., Isono, K., 1964. Lifetime of water drops before breaking and size distribution of fragment droplets. J. ,Metrorol. Soc. Japan 42, 330–340.
Lange, N.A., Forker, G.M., 1967. Handbook of Chemistry. McGraw-Hill, New York, p. 1998. Reference Volume For All Requiring Ready Access To Chemical & Physical Data. - Revised.
Langhans, M.H., Jaumann, R., Stephan, K., Brown, R.H., Buratti, B.J., Clark, R.N., Baines, K.H., Nicholson, P.D., Lorenz, R.D., Soderblom, L.A., Soderblom, J.M., 2012. Titan's fluvial valleys: morphology, distribution, and spectral properties. Planet. Space Sci. 60 (1), 34–51.
Laws, J., Parsons, D., 1943. The relation of raindrop-size to intensity, II. Trans. Am. Geophys. Union 24, 452–460.
Lohse, K.A., Deitrich, W.E., 2005. Contrasting effects of soil development on hydrological properties and flow paths. Water Resour. Res. 41, 12419. doi:10.1029/2004WR003403.
Lorenz, R.D., 1993. The life, death and afterlife of a raindrop on Titan. Planet. Space Sci. 41 (9), 647–655.
Lorenz, R.D., 2000. The weather on Titan. Science 290, 467–468.
Lorenz, R.D., Lunine, J.I., 1996. Erosion on Titan: past and present. Icarus 122, 79–91.
Lull, H.W., 1959. Soil Compaction on Forest and Range Lands. U.S. Dept. of Agriculture, Forestry Service Misc. Publication No.768.
Marshall, J.S., Palmer, W.M., 1948. The distribution of raindrops with size. J. Meteorol. 5, 165–166.
Matsubara, Y., Howard, A.D., 2013. Hydrology of early Mars: II.: valley network incision. J. Geophys. Res. 118, 1365–1387.
Matsubara, Y., Howard, A.D., Drummond, S.A., 2011. Hydrology of early Mars: lake basins. J. Geophys. Res. 116. doi:10.1029/2010JE003739.
Matsubara, Y., Howard, A.D., Gochenour, J.P., 2013. Hydrology of early Mars: valley network incision. J. Geophys. Res. 118, 1–23. doi:10.1002/jgre.20081.
Matthews, J.B., Mason, B.J., 1964. Electrification produced by the rupture of large water drops in an electric field. Q. J. Roy. Meteorol. Soc. 90, 275–286.
Moore, J.M., Howard, A.D., 2005. Large alluvial fans on Mars. J. Geophys. Res. 110, E04005.
Muller, C.J., Back, L.E., O'Gorman, P.A., Emanuel, K.A., 2009. A model for the relationship between tropical precipitation and column water vapor. Geophys. Res. Lett. 36 (16). doi:10.1029/2009GL039667.
Neris, J., Tejedor, M., Jimeńez, C., 2013. Soil properties controlling infiltration in volcanic soils. Geophys. Res. Abstr. 15 EGU2013-624-2.
Nutman, A.P., Mojzsis, S.J., Friend, C.R.L., 1997. Recognition of > 3850 Ma water-lain sediments and their significance for the early Archaean Earth. Geochimica et Cosmochimica Acta 61, 2475–2484.
Perron, J.T., Lamb, M.P., Koven, C.D., Fung, I.Y., Yager, E., Ádámkovics, M., 2006. Valley formation and methane precipitation rates on Titan. J. Geophys. Res.-Planets 111 (E11). doi:10.1029/2005JE002602.
Reyssat, E., Chevy, F., Biance, A.-L., Petitjean, L., Quere, D., 2007. Shape and instability of free-falling liquid globules. Europhys. Lett. 80, 34005.
Sagan, C., Mullen, G., 1972. Earth and Mars: evolution of atmospheres and surface temperatures. Science 177 (4043), 52–56.

Salles, C., Poesen, J., Govers, G., 2000. Statistical and physical analysis of soil detachment by raindrop impact: rain erosivity indices and threshold energy. Water Resour. Res. 36 (9), 2721–2729.
Segura, T.L., Toon, O.B., Colaprete, A., 2008. Modeling the environmental effects of moderate-sized impacts on Mars. J. Geophys. Res. 113, E11007.
Shin, S.S., Park, S.D., Choi, B.K., 2015. Universal power law for relationship between rainfall kinetic energy and rainfall intensity. Adv. Meteorol. Article ID **807973**.
Slate, J.L., Bull, W.B., Ku, T-.L., Shafiqullah, M., Lynch, D.L., Huang, Y-.P., 1991. Soil–carbonate genesis in the Pinacate volcanic field, Northwestern Sonora, Mexico. Quat. Res. 35, 400–416.
Som, S., Catling, D., Harnmeijer, J., Polivka, P., Buick, R., 2012. Air density 2.7 billion years ago limited to less than twice present levels by fossil raindrop imprints. Nature 484, 359–362.
Springer, G.S., 1976. Erosion by Liquid Impact. John Wiley and Sons, New York, p. 264.
Tokano, T., Molina-Cuberos, G.J., Lammer, H., Stumptner, W., 2001. Modelling of thunderclouds and lightning generation on Titan. Planet. Space Sci. 49 (6), 539–560.
Van Dijk, A., Bruijnzeel, L., Rosewell, C., 2002. Rainfall intensitykinetic energy relationships: a critical literature appraisal. Journal of Hydrology 261, 1–23. doi:10.1016/S0022-1694(02)00020-3.
Weislogel, M.M., Azzam, M.O.J., Mann, J.A., 1998. Effect of Gravity on Surface Tension, p. 3.
Williams, R.E.B., et al., 2013. Martian fluvial conglomerates at Gale Crater. Science 340, 1068–1072.
Wordsworth, R.D., Kerber, L., Pierrehumbert, R.T., Forget, F., Head III, J.W., 2015. Comparison of “warm and wet” and “cold and icy” scenarios for early Mars in a 3-D climate model. J. Geophys. Res. Planets 120, 1201–1219.
Young, R.A., Wierma, J.L., 1973. The role of rainfall impact in soil detachment and transport. Water Resour. Res. 9, 1629–1636.
Zanchi, C., Torri, D., 1980. Evaluation of rainfallenergy in central Italy. In: De-Boodt, M., Gabriels, D. (Eds.), Assessment of Erosion. John Wiley and Sons, Toronto, ON, pp. 133–142.
Zolotov, M.Yu., Mironenko, M.V., 2016. Chemical models for martian weathering profiles: insights into formation of layered phyllosilicate and sulfate deposits. Icarus 275, 203–220.